
Distribution of potentially toxic elements and health risk assessment of road dust in a steel industrial area

Albuja M. ^{1,2}, Jeong Hyeryeong ^{1,3,*}, Ra K. ^{1,2}

¹ Korea Institute of Ocean Science and Technology (KIOST), Marine Environmental Research Center, Busan, 49111, Republic of Korea

² Department of Ocean Science (Oceanography), KIOST School, University of Science and Technology (UST), Daejeon, 34113, Republic of Korea

³ Ifremer, RBE/CCEM, 44000, Nantes, France

* Corresponding author : Jeong Hyeryeong, email address : hrjeong617@gmail.com

Abstract :

The purpose of this study was to address the spatial distribution and the health risk of potentially toxic elements (Cr, Ni, Cu, Zn, As, Cd, Pb, and Hg) in different particle sizes of road dust samples from an industrial area of Pohang, South Korea. Concentrations in the six particle size fractions revealed a precise increasing order with decreasing particle size, with the highest average concentration in the [$< 63 \mu\text{m}$] particle size fraction for Zn (6161 mg/kg) and Cr (5225 mg/kg). In the [$< 63 \mu\text{m}$] particle size fraction, the mean values of the geoaccumulation index were found in the decreasing order: Zn \approx Cd (5.4) > Cr (5.1) > Pb (4.1) > Cu \approx Hg (3.3) > Ni (2.3) > As (0.3), and exceeded 4 in all sizes for Cr, showing a high to extremely high pollution status. It seems to be related to chromium plating and stainless alloy containing Cr in the steel industry process. Non-carcinogenic risk was found in Cr for children, while carcinogenic risk was found unacceptable for Ni, As, and Cd in children and for As and Ni in adults. The location of the study area near industrial, residential, and coastal areas makes its road dust pollution a combined threat to the human health and the marine environment. This study provides a basis for the improvement in pollution prevention and control strategies to reduce the environmental impact of potentially toxic metal contamination in road dust, as well as a road dust management insight in coastal industrial areas.

Keywords : Metal pollution, Size fractionation, Industry pollution, Road dust management

1. Introduction

Potentially toxic elements (PTEs) are considered as major environmental pollutants due to their toxicity, bioaccumulation, and non-degradability potential (Gbadamosi et al. 2018). The deposition of PTEs from the atmosphere can cause adverse effects on the ecosystem (Lazo et al. 2019). Besides, trace elements such as Cd, Pb, and As have exhibited adverse effects on human health even at low concentrations (Liu et al. 2021; Abdul et al. 2015). PTEs emitted from anthropogenic activities are prone to accumulation in soils, road dust, and plants (Men et al. 2018; Peng et al. 2020). In road dust, PTEs from different sources can accumulate through processes such as interception, deposition, and impaction (Wahab et al. 2020). It has been noted that PTEs can accumulate and be transferred to the food chain more easily from road dust than from soil (Khademi et al. 2019). Hence, road dust can be an appropriate indicator for assessing environmental pollution in urban areas (Ermolin et al. 2018; Heidari et al. 2021).

The composition of road dust is highly determined by emissions from surrounding areas (Lanzerstorfer and Logiewa 2019). Traffic activities, construction, fuel combustion, and the use of fertilizers and pesticides have been considered as important contributors to PTEs pollution through road dust (Men et al. 2020). However, industrial activities could have a greater impact on the environment (Jeong et al. 2020). It has been reported in several studies that industrial activities result in higher PTEs pollution than that of other anthropogenic activities such as agriculture or traffic (Men et al. 2021a; Xu et al. 2018; Hsu et al. 2021).

Fine-sized particles of road dust contain higher concentrations of PTEs than coarse-sized particles (Khademi et al. 2019; Jayarathne et al. 2017). Moreover, fine-sized particles of road dust are considered a serious threat to the environment as they are more easily resuspended after deposition (Cai et al. 2021). Fine and ultra-fine dust particles have a high potential to contain significant amounts of PTEs and to be resuspended in the environment and are of a great concern because they are more prone to human inhalation (Ramírez et al. 2020; Goix et al. 2014). Therefore, health risk assessment of PTEs in road dust is a public concern towards environment protection and population's health management. The increasing urbanization worldwide has reached a serious point where more than half the population lives in urban areas (Liu et al. 2019). This has led people to be constantly exposed to PTEs through road dust, posing a risk not only to the environment but also to human health (Safiur Rahman et al. 2019; Jayarathne et al. 2018). Prolonged exposure to PTEs might lead to carcinogenic and non-carcinogenic effects on humans (Ma et al. 2017). Numerous studies indicate that among general inhabitants, children are reportedly the most prone to health risks from PTEs in road dust (Qadeer et al. 2020; Wahab et al. 2020; Zheng et al. 2020). Moreover, a study conducted in Urumqi (NW, China) showed that while there was a carcinogenic and non-carcinogenic risk for children in soil and dust, the highest carcinogenic risk was found in dust (Peng et al. 2020). In view of this situation, for this study, road dust samples were collected from roads of residential areas next to the Pohang industrial complex in South Korea on October, 2013.

The objectives of this study are: (i) to investigate the concentration levels of PTEs in particle size fractions in road dust of an industrial site of South Korea; (ii) to characterize the spatial variation of PTEs in different particle fractions; and (iii) to assess the pollution status and (iv) health risk (carcinogenic risk and non-carcinogenic risk) posed by PTEs in road dust.

2. Materials and methods

2.1. Study area

Pohang (35°50′ – 36°20′ N, 128°59′ – 129°35′ E), located in the southern coast of South Korea, is home of one of the largest steel industries of the world (Kim et al. 2019; Park et al. 2021). The industrial area of Pohang is situated in the south of Hyungsan river, where metallic, non-ferrous metallic, chemical, petrochemical, electric, and electronic production, processing, or manufacturing activities take place (Baek et al. 2020). Pohang is also a populated coastal city of the North Gyeongsang Province (Lee et al. 2017). In fact, the industrial area, mainly specialized in iron-steel production, was built next to a sandy beach near residential areas, reason why civil complaints of pollution have been persistent since the 1990s (Baek et al. 2020). The map of the study area and the sampling sites are shown in Fig. 1.

2.2. Sampling

Road dust samples were collected from 19 sampling sites along roads of several neighborhoods in the Nam-gu district, next to a major steel industrial complex. Four or more subsamples were collected at each sampling site following a 10-day dry period. A vacuum cleaner (DC-35, Dyson, UK) was used to collect dust from the road surface. The samples were taken to the laboratory where they were dried at 40° in an oven, weighted, and stored in zip-lock bags until analysis. As a first step, large roots and leaves were removed by hand from the samples. Each road dust sample was sieved using a nylon sieve and vibratory sieve shaker (Analysette 3 pro, Fritsch Co., Germany) and divided into six different sizes ([<63 μm], [63-125 μm], [125-250 μm], [250-500 μm], [500-1000 μm] and [>1000 μm]).

2.3. PTEs analysis

Road dust samples were grinded and homogenized with a mechanical mortar (Pulverisette 6, Germany). The samples were digested for 24 hours at 180° in a mixture of hydrofluoric, nitric, and perchloric acid (5:4:1; Suprapur® grade). When dried, dissolution was performed using 1% (v/v) nitric acid. The PTEs concentrations were determined by an inductively coupled plasma mass spectrometry (ICP-MS; iCAP Q, Thermo Fisher Scientific, Germany). The concentration of mercury (Hg) was measured by an automated direct Hg analyzer (Hydra-C, USA) following the USEPA 7473 method. The certified reference materials MESS-4 and PACS-3 (National Research Council, Canada) were used to check data accuracy. The recoveries of PTEs ranged from 100.2 (Cu)% to 111.0 (Cd)%.

2.4. PTEs pollution assessment

In this study, in order to estimate the pollution levels of PTEs in size-fractionated road dust, pollution index was used. PTEs contamination is frequently evaluated by the geoaccumulation index (I_{geo}) (Muller 1969; Jeong et al. 2021):

$$I_{geo} = \log \left(\frac{C_n}{1.5 \times B_n} \right)$$

where, C_n and B_n represent the concentration of road dust and the background value (Rudnick and Gao 2003). The number of 1.5 is a factor used for background matrix correction. I_{geo} is divided into seven categories: no pollution [$I_{geo} < 0$]; no pollution to moderate pollution [$0 < I_{geo} < 1$]; moderate pollution [$1 < I_{geo} < 2$]; moderate to high pollution [$2 < I_{geo} < 3$]; high pollution [$3 < I_{geo} < 4$]; high to extremely high pollution [$4 < I_{geo} < 5$]; and extremely high pollution [$I_{geo} > 5$].

The overall contamination level for PTEs in this study was evaluated using pollution load index (PLI):

$$PLI = (PI_1 \times PI_2 \times PI_3 \dots \times PI_n)^{1/n}$$

where, PI represents the ratio of PTEs between road dust and the background value and n is the number of PTEs analyzed. A PLI value greater than 1 indicates the presence of PTEs contamination.

2.5. Health risk assessment

For the health risk assessment of this study, the [$< 63 \mu m$] particle size fraction of road dust was considered. The average daily dose (ADD) was used to calculate the health risk posed on adults and children by PTEs in road dust in the study area. The three exposure pathways (ingestion, inhalation, and dermal contact) are considered as follows (USEPA 2011a):

$$ADD_{ing} = C_i \times \left(\frac{IngR \times EF \times ED}{BW \times AT} \right) \times 10^{-6}$$

$$ADD_{inh} = C_i \times \left(\frac{InhR \times EF \times ED}{PEF \times BW \times AT} \right)$$

$$ADD_{dermal} = C_i \times \left(\frac{SL \times SA \times ABS \times EF \times ED}{BW \times AT} \right) \times 10^{-6}$$

where C_i is the PTEs concentration in road dust; IngR is the ingestion rate of road dust; ED and EF represent the exposure duration and frequency; BW is the body weight; AT is the average time of exposure; InhR is the rate of inhalation of road dust; PEF is particle emission factor; SA is the surface area of skin in humans that is exposed to road dust; SL and ABS are the dermal adherence and dermal absorption factors. Reference values and units are listed in Table S1.

Non-carcinogenic risk is calculated with respect to the average daily doses in the previous step:

$$HQ_i = \frac{ADD_i}{R_f D}$$

$$HI = \sum_{i=1}^p HQ_i$$

where HQ_i is the hazard quotient attributed to each route, ADD_i is the average daily dose, and $R_f D$ is the reference dose. HI is the hazard index, which represents the non-carcinogenic risk of each route (ingestion, inhalation, and dermal contact). Non-carcinogenic risk is possible at $HI > 1$ and its probability increases with increasing HI value (USEPA 2001).

The carcinogenic risk posed by PTEs was calculated as follows:

$$CR_{ing} = ADD_{ing} \times SF$$

$$CR_{inh} = ADD_{inh} \times IUR$$

$$CR_{derm} = ADD_{derm} \times (SF_o/GIABS)$$

where SF is the carcinogenic slope factor of individual PTEs, IUR is the inhalation unit risk, and GIABS is the gastrointestinal absorption factor. The values were obtained from [USEPA \(2011b\)](#). Cancer risk is negligible at $CR < 10^{-6}$, unacceptable at $CR > 10^{-4}$, and tolerable for values in between ([USEPA 2002](#)). Reference doses and slope factors are obtained from [Ferreira-Baptista and de Miguel \(2005\)](#) and [Ma et al. \(2019\)](#).

3. Results and discussion

3.1. Concentration levels and spatial distribution of PTEs in road dust

The mean PTEs concentrations (mg/kg) of all particle size fractions over all the study areas were found in the following order: Cr (3738 mg/kg) > Zn (2364.8 mg/kg) > Cu (336.6 mg/kg) > Pb (307.9 mg/kg) > Ni (228.2 mg/kg) > As (17.2 mg/kg) > Cd (3.62 mg/kg) > Hg (0.80 mg/kg) ([Table 1](#)). Similarly, the highest PTEs concentrations in this study were assigned to the [$<63 \mu\text{m}$] particle size fraction of Zn (6161.4 mg/kg) and Cr (5225 mg/kg). Based on the total PTEs concentrations (Cr, Ni, Cu, Zn, As, Cd, Pb, Hg) of all sites, the particle size fractions could be classified as follows: [$<63 \mu\text{m}$] > [$63\text{-}125 \mu\text{m}$] > [$125\text{-}250 \mu\text{m}$] > [$250\text{-}500 \mu\text{m}$] > [$>1000 \mu\text{m}$] > [$500\text{-}1000 \mu\text{m}$]. With the exception of [>1000] fraction, there is an increasing PTEs concentration with decreasing particle size. This suggests an overall higher concentration of PTEs in finer particle size fractions of road dust. [Lanzerstorfer and Logiewa \(2019\)](#) analyzed urban road dust in the city of Kleszczów and obtained similar results, where the highest concentration of PTEs was found in the finest particle size fractions of road dust. This is because the absorption capacity of finer particles is relatively higher than that of larger particles ([Jayarathne et al. 2017](#)).

[Table 1](#) shows a comparison of the average concentrations of PTEs in road dust of this study with those of other international cities. The concentrations of As and Cd in this study were lower than those of Viana do Castelo (Portugal; [Alves et al. 2020](#)); Dhaka (Bangladesh; [Safiur Rahman et al. 2019](#)) and Jeddah (Saudi Arabia; [Shabbaj et al. 2018](#)), respectively. For the rest of concentrations, the highest values of this study are considerably higher than those in other international cities ([Huainan; Liu et al. 2021](#), [Delhi; Suryawanshi 2016](#), and [Tongchuan; Lu et al. 2017](#)). The mean concentrations of the smallest fraction of road dust in this study were found to be 56.7 times greater for Cr and 22.6 times greater for Ni compared to the mean concentrations of the same size fraction of road dust in the urban city of Busan, South Korea. Lower concentrations of Ni, Cu, Zn, As, Cd, and Hg were found in the study area compared to the smelter industrial area of Onsan, South Korea. Cd and As were found to be similar to those in other urban cities. Notably, there is significantly higher accumulation of Cr in the industrial area of Pohang relative to other cities, even to the ones affected by industrial activities.

The average concentration of Zn in the <63 μm size fraction of road dust (6161.4 mg/kg) was higher than those of the soil pollution concern and countermeasure standards of road and factories in South Korea (Table 1). In the case of the other PTEs, the average PTEs concentrations show lower values than those of the concern and countermeasure quality standards. Nonetheless, several sampling points presented concentrations substantially higher than those of the quality standards. For instance, while the average concentration of Pb (644.5 mg/kg) in the finest size fraction of road dust is lower than the soil pollution standards, its maximum concentration (3850 mg/kg) was found to be as high as 5 times the concern standard (700 mg/kg) and 1.8 times the countermeasure standard (2100 mg/kg). Hence, the analysis of the spatial variation of PTEs in road dust of the study area is important.

The site with the highest total PTEs concentration was site PH-9, which exhibited especially high concentrations of Zn (32379.0 mg/kg) and Cr (4032 mg/kg) in the [<63 μm] particle size fraction. Sampling sites PH-7 and PH-12 followed, with high concentrations in the [<63 μm] particle size fraction of Zn (18923.7 mg/kg) and Cr (12162 mg/kg), respectively. The sites with the lowest concentrations were PH-4 and PH-3, located in the western part of the study area. Nonetheless, the highest concentrations in these sites were also found in the [<63 μm] particle size fraction of the road dust sample. Given that the PTEs accumulation was especially significant in this particle size fraction for most of the sampling sites, the spatial distribution of the PTEs concentrations in road dust was analyzed for the [<63 μm] particle size fraction in Fig. 2. The variation of the prominent PTEs in each area might be related to the presence of an industry close to the sampling point. Baek et al. (2020) addressed the air pollution of a residential area near an iron-steel industry in Pohang, and found that these activities had a great impact on the PTEs levels in airborne particles, and that their concentration varied spatially. Thus, different industries in the study area may be responsible of the contamination in road dust by different PTEs. As shown in Fig. 2, there was higher concentration of Cr and Cu in the northern part of the study area than that on the central and southern. Nearby, an important iron-steel manufacturing company was located. It has been reported that in the process of steel making, Cr is useful for corrosion resistance (Mandalika et al. 2022), and Co for strength and ductility (Kim et al. 2021). Likewise, in the central part of the study area, especially along the sampling site PH-12, higher concentrations of Cr, As, Cd and Hg, were found. In this area, two automotive businesses mainly focused on the development and manufacturing of automobiles were located. In the southern part of the study area, there was high concentration of Ni, Zn, and Pb, where automobile and heavy machinery rental services were found. Ashraf et al. (2020) associated emissions from automobile workshops to excessive amounts of Zn, Cr, Pb, and Ni in groundwater. Likewise, given that PTEs with high concentrations and bioaccessibility can accumulate in road dust from processes such as tire wear and diesel engine exhaust (Hong et al. 2020), the extremely high concentration of Zn in PH-9 could be related to the excessive automobile activities in the area. Therefore, the large PTEs amounts found in road dust near small and large industries in Pohang require emissions regulations to be addressed immediately.

3.2. Pollution assessment of PTEs

The calculated I_{geo} values, presented in Table 2, were considered to substantiate the correlation between

particle size fraction and PTEs contamination in road dust. The finest road dust (<63 µm) had the highest I_{geo} values for PTEs except for As. The highest mean I_{geo} values for less than 63 µm were found in Cr (5.1), followed by Ni (2.3), Cu (3.3), Zn (5.4), Cd (5.4), Pb (4.1), and Hg (3.3). The finest particle of road dust is characterized with extremely high pollution for Cr, Zn, and Cd. The finest road dust presented high to extremely high pollution for Pb, high pollution for Cu and Hg, and moderate to high pollution for Ni.

In the case of Cr, the mean I_{geo} values exceeded 4 in all sizes of road dust and the finest road dust with 53% for [>1000 µm] and [250-500 µm], 37% for [500-1000 µm], 74% for [125-250 µm], 89% for [63-125 µm] and [<63 µm] exceeded the I_{geo} values of 4, indicating high to extremely high pollution. For less than 125 µm, two sampling sites (PH-4 and PH-8) had I_{geo} values between 3 and 4, which showed a high pollution level. Zn and Cd showed extremely high pollution with an average I_{geo} of 5.4 for [<63 µm] road dust particle fraction. In sizes [125-250 µm] and [63-125 µm], I_{geo} showed high to extremely high pollution for Zn and Cd. For Cu, particles larger than 125 µm showed moderate to high pollution with I_{geo} values between 2 and 3, but particles less than 125 µm indicated high pollution with a mean I_{geo} value of more than 3. For Pb, [<63 µm] presented high to extremely high pollution, [63-250 µm] high pollution, [250-1000 µm] moderate to high pollution, and [>1000 µm] showed moderate pollution. As the particle size became smaller, the pollution level seriously increased. For As, I_{geo} values in all particle sizes showed that the road dust was in the no pollution to moderate pollution category ($0 < I_{geo} < 1$). The results of I_{geo} values indicated that Cr, Cu, Zn, Cd, and Pb in the fine road dust presented high pollution in steel industrial areas.

The mean pollution load index (PLI) values of all PTEs for each particle size fraction showed a clear increase with decreasing particle size as follows: [<63 µm] (21.8) > [63-125 µm] (16.9) > [125-250 µm] (11.5) > [250-500 µm] (9.1) > [500-1000 µm] (7.1) > [>1000 µm] (5.4). Even so, all the particle size fractions showed PLI values greater than 1, with values as high as 61.75 in road dust of [<63 µm] particle size. The spatial distribution of PLI for every particle size fraction is displayed in [Figure 3](#). The highest PLI values were found in the PH-12 site for all the particle sizes. Extremely high PLI values were also present in PH-11 and PH-10 for finer particle size fractions. Hence, the areas around these sampling sites showed the highest contamination in road dust in this study. The roads in these areas surround steel manufacturing, automotive and waste management industries, which could be attributed as the main sources of PTEs in road dust. The lowest PLI values were found in the northwestern part of the study area. Nonetheless, it cannot be disregarded given that PLI values surpass 1 in every sampling site, showing significant contamination in road dust throughout the entire industrial complex of the study area.

3.3. Health risk assessment ([<63 µm] particle size fraction)

3.3.1. Non-carcinogenic risk

[Table 3](#) shows that the hazard index (HI) for Cr in children and adults was higher than the safe value of 1 (1.4 and 7.8, respectively). The values for Ni, Cu, Zn, As, Cd, Pb, and Hg were less than 1, suggesting that there is no significant non-carcinogenic risk posed by these metals. The HI values for children were

consistently higher than those for adults, indicating a higher susceptibility on children to the effects of the exposure to PTEs in road dust. Likewise, [Wahab et al. \(2020\)](#) reported greater noncancerous risk for children than for adults, especially from Pb, as children have higher hand-to-mouth contact on surfaces that contains Pb-based paints or road dust. This has been confirmed by several studies, in which ingestion has been recognized as the main exposure pathway for children to PTEs in road dust ([Safiur Rahman et al. 2019](#); [Peng et al. 2020](#); [Zheng et al. 2020](#)). Similar results were obtained in this study. The highest quotient values were assigned to children's ingestion (HQ_{ing}) of Cr (5.7) followed by dermal absorption (HQ_{derm}) of Cr for children (1.6). Iron-steel industries, which are prominent in the study zone, usually use Cr for corrosion resistance in the process of steel manufacturing ([Mandalika et al. 2022](#)). Cr could be eventually emitted and accumulated in road dust. The high concentration of Cr in the samples led to the high HI reported in the study, and could signify deleterious health conditions in children as they are at risk of developing neurological and growth disorders as a result of the exposure to large quantities of Cr ([Ferreira-Baptista and De Miguel 2005](#)). Thus, Cr emissions should be more strictly regulated in order to prevent such affections in human health.

3.3.2. Carcinogenic risk

The cancer risk (CR) of As, Cd, Ni, and Pb is presented in [Table 4](#). Ni for adults and As, Cd, and Ni for children had CR values via ingestion (CR_{ing}) higher than 10^{-6} , the internationally accepted criterion for unacceptable CR levels ([Safiur Rahman et al. 2019](#)). Tolerable values were found in CR_{ing} of As, Cd, and Pb in adults and Pb in children, demonstrating that ingestion is too the main exposure pathway for cancer risk, especially for children. Negligible values were found in CR via inhalation (CR_{inh}) for the analyzed metals, revealing that there is a low probability of these metals to pose a risk to people to develop other type of cancer after lifetime exposure through inhalation of road dust in the study area. Tolerable CR values via dermal absorption (CR_{derm}) were found in As and Pb for both adults and children. A study that analyzed PM in Pohang detected the highest carcinogenic risk in As ([Baek et al. 2020](#)). In this study, As and Ni presented the highest HI values in adults (1.2×10^{-4} , and 1.1×10^{-4} , respectively) and children (9.7×10^{-4} , and 1.0×10^{-3} , respectively). Cd also showed an unacceptable HI value (3.7×10^{-4}) for children; revealing that As, Cd, and Ni have the highest possibilities among the analyzed PTEs of posing carcinogenic risk to human health in the study area. The International Agency for Research on Cancer (IARC) categorizes As, Cd, and Ni as class I carcinogenic elements ([Safiur Rahman et al. 2019](#)). Hence, lifetime exposure to these PTEs through road dust in the study area, especially via ingestion, could ultimately result in carcinogenic health effects.

3.4 Road dust management

In South Korea, 493 sections of 1972 km of road across the country have been designated as intensively managed roads, and a total of about 1650 road cleaning vehicles are being operated to reduce fine dust and sources of non-point pollution. However, road cleaning is mainly concentrated in urban cities because it is considered in terms of vehicle traffic and population, and road cleaning for industrial areas is still insufficient. Additionally, national industrial complexes, including the Pohang steel industrial complex of the study area, have been created in accordance with the heavy industry promotion policy

since the 1980s, and are still in active operation. Since the surrounding cities are built around industrial areas and there is a high risk that residents and workers may be exposed to PTEs in road dust, road cleaning for industrial areas should be strengthened.

Moreover, the management of PTEs in road dust of industrial areas could also be improved within the cleaning process. Since small size particles have shown the highest PTEs concentration and pollution risk due to their high absorption capacity, the removal of fine-size particles from the roads should be prioritized. Moreover, given that industrial areas such as the Pohang industrial complex present high concentrations of certain PTEs, the cleaning system of road dust could be directed to target these pollutants in particular. In this study, the highest concentrations were found for Zn and Cr, which also were the main PTEs present in the sampling areas with the overall highest concentration. Zn also presented a higher concentration than those of the soil pollution concern and countermeasure standards of South Korea. Cr presented extremely high pollution status according to I_{geo} , had a larger concentration when compared to other international cities and was found to pose non-carcinogenic risk to children via ingestion. I_{geo} also revealed concerning quantities of Zn and Cd, and the health risk assessment showed unacceptable carcinogenic risk for Ni, As, and Cd. The persistence of specific PTEs throughout the spatial variation and concentration, pollution and health risk analysis in this study could serve to target the concerning PTEs in the Pohang industrial complex and to identify the sources of their emissions.

For the purpose of managing the PTEs-containing road dust during the cleaning process, several fractionation technologies could be used. For instance, in a previous study done in Pohang (Jeong and Ra 2022a), the advantage of separating road dust by its magnetic properties was highlighted: the magnetic fraction of road dust particles accounted for more than 60% the metal load in the road dust samples. Thus, the development of a cleaning system that contemplates pollution influencing factors such as size and magnetism to improve the management of potentially contaminant road dust could be a relevant improvement towards the protection of the environment and the human health in industrial areas.

The location of the study area is a main aspect when considering the correct management of PTEs-containing road dust. The fact that a residential area is located next to the Pohang industrial complex is already a relevant aspect of consideration. As this study suggests, the fine-size particles of road dust have higher risk of contamination. These fine particles are also easily resuspended by wind, which could eventually reach residential areas, posing a risk to the health of Pohang citizens. Furthermore, the Pohang industrial complex is located in a coastal area where major import and export activities take place on a daily basis. Hence, the already compromised marine environment is at risk not only by the potential polluting emissions from ships, but also from the terrestrial watershed. The easy resuspension of fine-sized particles facilitates their transport towards rivers or directly to the ocean through runoff, potentially producing an adverse impact on marine organisms. Therefore, fine-sized road dust contaminated with PTEs is not only a serious threat to the human health when resuspended, but also to the marine biota in coastal areas. For this reason, the management of road dust should also be pointed towards the precise interruption of the transport of road dust particles towards residential and marine areas through wind and runoff.

4. Conclusions

In this study, the spatial variation and health risk assessment of PTEs in six particle size fractions of road dust in an industrial area of Pohang, South Korea were analyzed. High concentrations of Zn and Cr were found in the smallest particle size of road dust. Cr concentration was found to be larger than that of other urban and industrial cities, while Zn was found to have a larger concentration than those of the soil pollution concern and countermeasure standards of road and factory standards of South Korea. The accumulation of these PTEs in road dust, especially on sampling site PH-9, seems to be related to the heavy use of Cr for chromium plating and stainless alloy in steel manufacturing and of Zn for automobile fabrication in the Pohang industrial complex. PTE emissions could negatively affect human health, especially that of children, who were found to be the most susceptible to non-carcinogenic risk from Cr and to carcinogenic risk from Ni, As, and Cd in road dust via ingestion. The particle size of road dust was found to be significant when addressing PTEs contamination as different sizes tend to have different concentrations of PTEs, hence, are likely to pose different degrees of risk. Fine-sized road dust contamination is more likely to cause adverse effects on the human health and the marine environment as small particles could be easily transported to residential and coastal areas through wind and runoff. Special attention should be given to industries and their emissions as the critical sources of contamination in the region. Road dust management could be done during the cleaning process of roads through technologies targeting on particular PTEs and fractions of road dust, and by interrupting the transport of fine road dust particles towards water bodies. Lastly, in order to have a more comprehensive picture of human exposure to PTEs emissions from the industrial city of Pohang, in addition to road dust, investigation of the presence of PTEs in indoor dust, soil, groundwater and dairy intake is suggested for future studies.

Acknowledgments

This research was funded by the Korea Institute of Ocean Science and Technology (KIOST), grant number PEA0012.

References

- Abdul KSM, Jayasinghe SS, Chandana EPS, et al (2015) Arsenic and human health effects: A review. *Environ Toxicol Pharmacol* 40:828–846. <https://doi.org/10.1016/j.etap.2015.09.016>
- Alves CA, Vicente ED, Vicente AMP, et al (2020) Loadings, chemical patterns and risks of inhalable road dust particles in an Atlantic city in the north of Portugal. *Science of The Total Environment* 737:139596. <https://doi.org/10.1016/j.scitotenv.2020.139596>
- Ashraf S, Rizvi NB, Rasool A, et al (2020) Evaluation of heavy metal ions in the groundwater samples from selected automobile workshop areas in northern Pakistan. *Groundwater for Sustainable Development* 11:100428. <https://doi.org/10.1016/j.gsd.2020.100428>
- Baek K-M, Kim M-J, Kim J-Y, et al (2020) Characterization and health impact assessment of hazardous air pollutants in residential areas near a large iron-steel industrial complex in Korea. *Atmospheric Pollution Research* 11:1754–1766. <https://doi.org/10.1016/j.apr.2020.07.009>
- Cai Y, Li F, Zhang J, et al (2021) Toxic metals in size-fractionated road dust from typical industrial district: Seasonal distribution, bioaccessibility and stochastic-fuzzy health risk management. *Environmental Technology & Innovation* 23:101643. <https://doi.org/10.1016/j.eti.2021.101643>
- Ermolin MS, Fedotov PS, Ivaneev AI, et al (2018) A contribution of nanoscale particles of road-deposited sediments to the pollution of urban runoff by heavy metals. *Chemosphere* 210:65–75. <https://doi.org/10.1016/j.chemosphere.2018.06.150>
- Ferreira-Baptista L, De Miguel E (2005) Geochemistry and risk assessment of street dust in Luanda, Angola: A tropical urban environment. *Atmospheric Environment* 39:4501–4512. <https://doi.org/10.1016/j.atmosenv.2005.03.026>
- Gbadamosi MR, Afolabi TA, Ogunneye AL, et al (2018) Distribution of radionuclides and heavy metals in the bituminous sand deposit in Ogun State, Nigeria – A multi-dimensional pollution, health and radiological risk assessment. *Journal of Geochemical Exploration* 190:187–199. <https://doi.org/10.1016/j.gexplo.2018.03.006>
- Goix S, Lévêque T, Xiong T-T, et al (2014) Environmental and health impacts of fine and ultrafine metallic particles: assessment of threat scores. *Environ Res* 133:185–194. <https://doi.org/10.1016/j.envres.2014.05.015>
- Heidari M, Darijani T, Alipour V (2021) Heavy metal pollution of road dust in a city and its highly polluted suburb; quantitative source apportionment and source-specific ecological and health risk assessment. *Chemosphere* 273:129656. <https://doi.org/10.1016/j.chemosphere.2021.129656>
- Hong N, Guan Y, Yang B, et al (2020) Quantitative source tracking of heavy metals contained in urban road deposited sediments. *Journal of Hazardous Materials* 393:122362. <https://doi.org/10.1016/j.jhazmat.2020.122362>

- Hsu C-Y, Chi K-H, Wu C-D, et al (2021) Integrated analysis of source-specific risks for PM_{2.5}-bound metals in urban, suburban, rural, and industrial areas. *Environmental Pollution* 275:116652. <https://doi.org/10.1016/j.envpol.2021.116652>
- Jayarathne A, Egodawatta P, Ayoko GA, Goonetilleke A (2017) Geochemical phase and particle size relationships of metals in urban road dust. *Environmental Pollution* 230:218–226. <https://doi.org/10.1016/j.envpol.2017.06.059>
- Jayarathne A, Egodawatta P, Ayoko GA, Goonetilleke A (2018) Assessment of ecological and human health risks of metals in urban road dust based on geochemical fractionation and potential bioavailability. *Science of The Total Environment* 635:1609–1619. <https://doi.org/10.1016/j.scitotenv.2018.04.098>
- Jeong H, Choi JY, Lim J, Ra K (2020) Pollution Caused by Potentially Toxic Elements Present in Road Dust from Industrial Areas in Korea. *Atmosphere* 11:1366. <https://doi.org/10.3390/atmos11121366>
- Jeong H, Choi JY, Ra K (2021) Potentially toxic elements pollution in road deposited sediments around the active smelting industry of Korea. *Sci Rep* 11:7238. <https://doi.org/10.1038/s41598-021-86698-x>
- Jeong H, Ra K (2022a) Investigations of metal pollution in road dust of steel industrial area and application of magnetic separation. *Sustainability* 14:919. <https://doi.org/10.3390/su14020919>
- Jeong H, Ra K (2022b) Source apportionment and health risk assessment for potentially toxic elements in size-fractionated road dust in Busan Metropolitan City, Korea. *Environ Monit Assess* 194:350. <https://doi.org/10.1007/s10661-022-10008-9>
- Khademi H, Gabarrón M, Abbaspour A, et al (2019) Environmental impact assessment of industrial activities on heavy metals distribution in street dust and soil. *Chemosphere* 217:695–705. <https://doi.org/10.1016/j.chemosphere.2018.11.045>
- Kim H, Park C, Park M-H, Song Y (2019) Diagenetic study on the Neogene sedimentary basin as paleoenvironmental proxy data for an offshore CO₂ storage project in Pohang Basin, South Korea. *Marine Geology* 416:105977. <https://doi.org/10.1016/j.margeo.2019.105977>
- Kim K-S, Kim Y-K, Yang S, et al (2021) Microstructure and mechanical properties of carbon-bearing ultrahigh-strength high Co-Ni Steel (AerMet 340) fabricated via laser powder bed fusion. *Materialia* 20:101244. <https://doi.org/10.1016/j.mtla.2021.101244>
- Lanzerstorfer C, Logiewa A (2019) The upper size limit of the dust samples in road dust heavy metal studies: Benefits of a combined sieving and air classification sample preparation procedure. *Environmental Pollution* 245:1079–1085. <https://doi.org/10.1016/j.envpol.2018.10.131>
- Lazo P, Stafilov T, Qarri F, et al (2019) Spatial distribution and temporal trend of airborne trace metal deposition in Albania studied by moss biomonitoring. *Ecological Indicators* 101:1007–1017. <https://doi.org/10.1016/j.ecolind.2018.11.053>

- Lee J, Lee J, Hong S, et al (2017) Characteristics of meso-sized plastic marine debris on 20 beaches in Korea. *Marine Pollution Bulletin* 123:92–96. <https://doi.org/10.1016/j.marpolbul.2017.09.020>
- Liu E, Wang X, Liu H, et al (2019) Chemical speciation, pollution and ecological risk of toxic metals in readily washed off road dust in a megacity (Nanjing), China. *Ecotoxicology and Environmental Safety* 173:381–392. <https://doi.org/10.1016/j.ecoenv.2019.02.019>
- Liu Y, Liu G, Yousaf B, et al (2021) Identification of the featured-element in fine road dust of cities with coal contamination by geochemical investigation and isotopic monitoring. *Environment International* 152:106499. <https://doi.org/10.1016/j.envint.2021.106499>
- Lu X, Pan H, Wang Y (2017) Pollution evaluation and source analysis of heavy metal in roadway dust from a resource-typed industrial city in Northwest China. *Atmospheric Pollution Research* 8:587–595. <https://doi.org/10.1016/j.apr.2016.12.019>
- Ma L, Abuduwaili J, Liu W (2019) Spatial Distribution and Health Risk Assessment of Potentially Toxic Elements in Surface Soils of Bosten Lake Basin, Central Asia. *International Journal of Environmental Research and Public Health* 16:3741. <https://doi.org/10.3390/ijerph16193741>
- Ma L, Wang L, Tang J, Yang Z (2017) Arsenic speciation and heavy metal distribution in polished rice grown in Guangdong Province, Southern China. *Food Chemistry* 233:110–116. <https://doi.org/10.1016/j.foodchem.2017.04.097>
- Mandalika BVR, Annamraju S, Nayaka N (2022) Development of seismic resistant steel with high strength and corrosion resistance. *Materials Today: Proceedings*. <https://doi.org/10.1016/j.matpr.2022.01.434>
- Men C, Liu R, Xu F, et al (2018) Pollution characteristics, risk assessment, and source apportionment of heavy metals in road dust in Beijing, China. *Science of The Total Environment* 612:138–147. <https://doi.org/10.1016/j.scitotenv.2017.08.123>
- Men C, Liu R, Xu L, et al (2020) Source-specific ecological risk analysis and critical source identification of heavy metals in road dust in Beijing, China. *Journal of Hazardous Materials* 388:121763. <https://doi.org/10.1016/j.jhazmat.2019.121763>
- Men C, Liu R, Wang Q, et al (2021a) Spatial-temporal characteristics, source-specific variation and uncertainty analysis of health risks associated with heavy metals in road dust in Beijing, China. *Environmental Pollution* 278:116866. <https://doi.org/10.1016/j.envpol.2021.116866>
- Ministry of Government Legislation (MGL) (2019) Korea soil quality standard of heavy metals in soil environment conservation act (Law No.16613).
- Muller G (1969) Index of geoaccumulation in sediments of the Rhine River. *Geojournal* 2:108-118.
- Park M-K, Cho H-K, Cho I-G, et al (2021) Contamination characteristics of polychlorinated naphthalenes in the agricultural soil of two industrial cities in South Korea. *Chemosphere* 273:129721. <https://doi.org/10.1016/j.chemosphere.2021.129721>

Peng L, Li X, Sun X, et al (2020) Comprehensive Urumqi screening for potentially toxic metals in soil-dust-plant total environment and evaluation of children's (0–6 years) risk-based blood lead levels prediction. *Chemosphere* 258:127342. <https://doi.org/10.1016/j.chemosphere.2020.127342>

Qadeer A, Saqib ZA, Ajmal Z, et al (2020) Concentrations, pollution indices and health risk assessment of heavy metals in road dust from two urbanized cities of Pakistan: Comparing two sampling methods for heavy metals concentration. *Sustainable Cities and Society* 53:101959. <https://doi.org/10.1016/j.scs.2019.101959>

Ramírez O, da Boit K, Blanco E, Silva LFO (2020) Hazardous thoracic and ultrafine particles from road dust in a Caribbean industrial city. *Urban Climate* 33:100655. <https://doi.org/10.1016/j.uclim.2020.100655>

Rudnick R, Gao S (2003) Composition of the Continental Crust. *Treatise on Geochemistry* 3:1–64. <https://doi.org/10.1016/B0-08-043751-6/03016-4>

Safiur Rahman M, Khan MDH, Jolly YN, et al (2019) Assessing risk to human health for heavy metal contamination through street dust in the Southeast Asian Megacity: Dhaka, Bangladesh. *Science of The Total Environment* 660:1610–1622. <https://doi.org/10.1016/j.scitotenv.2018.12.425>

Shabbaj II, Alghamdi MA, Shamy M, et al (2018) Risk Assessment and Implication of Human Exposure to Road Dust Heavy Metals in Jeddah, Saudi Arabia. *International Journal of Environmental Research and Public Health* 15:36. <https://doi.org/10.3390/ijerph15010036>

Suryawanshi PV, Rajaram BS, Bhanarkar AD, Rao CVC (2016) Determining heavy metal contamination of road dust in Delhi, India. *Atmósfera* 29:221–234. <https://doi.org/10.20937/ATM.2016.29.03.04>

USEPA (U.S. Environmental Protection Agency) (2001) Risk assessment guidance for superfund. In: Part A, Process for Conducting Probabilistic Risk Assessment. vol. III. EPA 540-R-02–002. Office of Emergency and Remedial Response, Washington, DC, USA.

USEPA (U.S. Environmental Protection Agency) (2002) Child-specific exposure factors handbook. EPA-600-P-00–002B. National Center for Environmental Assessment. Washington, DC. USA.

USEPA (U.S. Environmental Protection Agency) (2011a) Exposure Factors Handbook (Final), 584 EPA/600/R-09/052F, Washington, DC, USA.

USEPA (U.S. Environmental Protection Agency) (2011b) The screening level (RSL) tables. <https://www.epa.gov/risk/regional-screening-levels-rsls-generic-tables>. Accessed 16 May 2022

Wahab MIA, Razak WMAA, Sahani M, Khan MF (2020) Characteristics and health effect of heavy metals on non-exhaust road dusts in Kuala Lumpur. *Science of The Total Environment* 703:135535. <https://doi.org/10.1016/j.scitotenv.2019.135535>

Xu D-M, Zhang J-Q, Yan B, et al (2018) Contamination characteristics and potential environmental implications of heavy metals in road dusts in typical industrial and agricultural cities, southeastern

Hubei Province, Central China. *Environ Sci Pollut Res Int* 25:36223–36238. <https://doi.org/10.1007/s11356-018-3282-6>

Zheng N, Hou S, Wang S, et al (2020) Health risk assessment of heavy metals in street dust around a zinc smelting plant in China based on bioavailability and bioaccessibility. *Ecotoxicology and Environmental Safety* 197:110617. <https://doi.org/10.1016/j.ecoenv.2020.110617>

[List of figures]

Fig.1. Study area and sampling sites in an industrial area of Pohang, South Korea.

Fig. 2. Spatial distribution of PTEs in road dust (<63 μm) from the industrial complex area of Pohang, South Korea.

Fig. 3. PLI distribution of each particle size fraction of road dust from the industrial complex area of Pohang, South Korea.

[List of tables]

Table 1. Comparison of average PTEs concentrations (mg/kg) (minimum and maximum concentrations in parentheses) in different particle sizes of road dust in this study and those in other published data.

Table 2. Classification of the pollution levels using mean Igeo values for PTEs in six particle size fractions of road dust in this study.

Table 3. Non-carcinogenic health risk assessment in the [<63 μm] size fraction of road dust in this study.

Table 4. Carcinogenic health risk assessment in the [<63 μm] size fraction of road dust in this study.

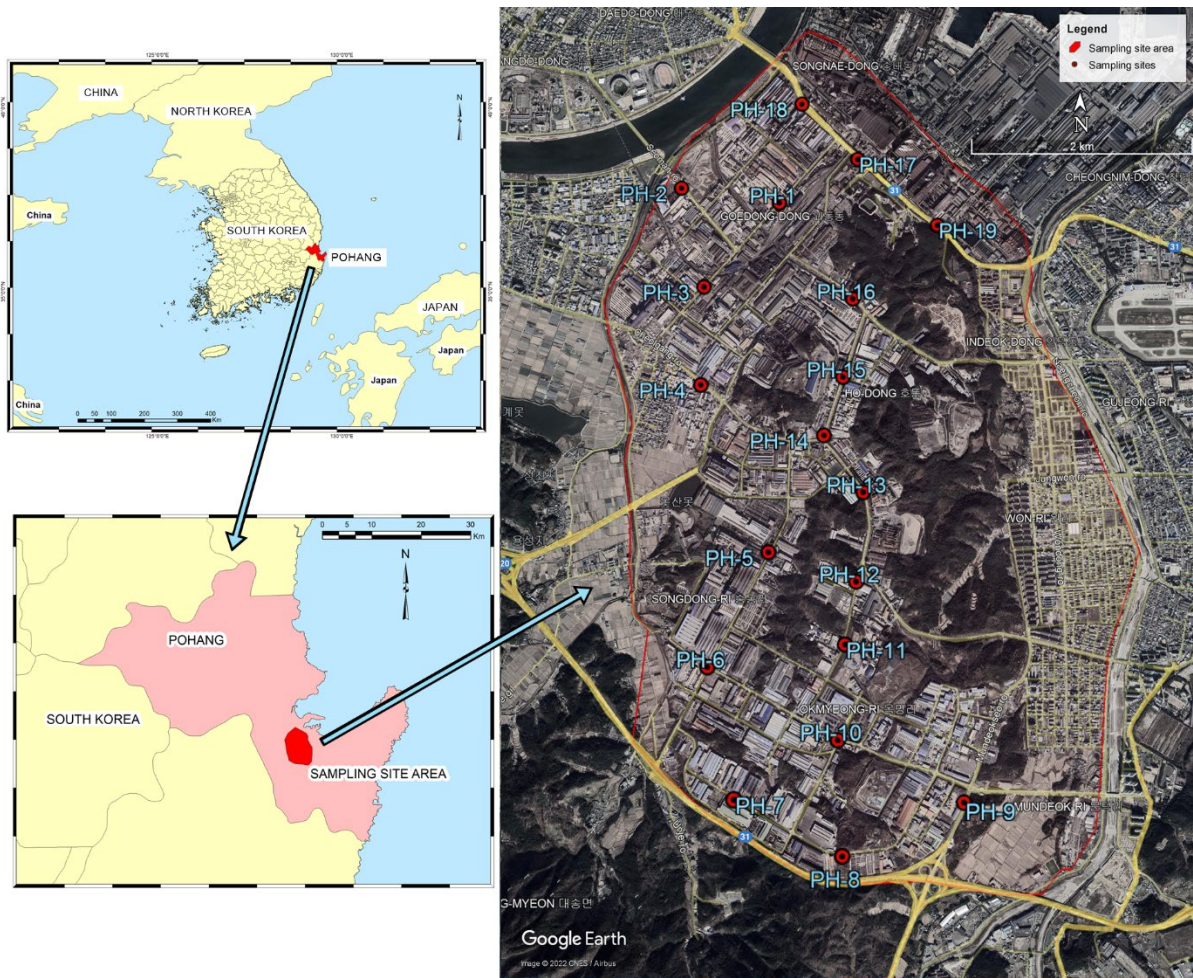


Fig.1. Study area and sampling sites in an industrial area of Pohang, South Korea.

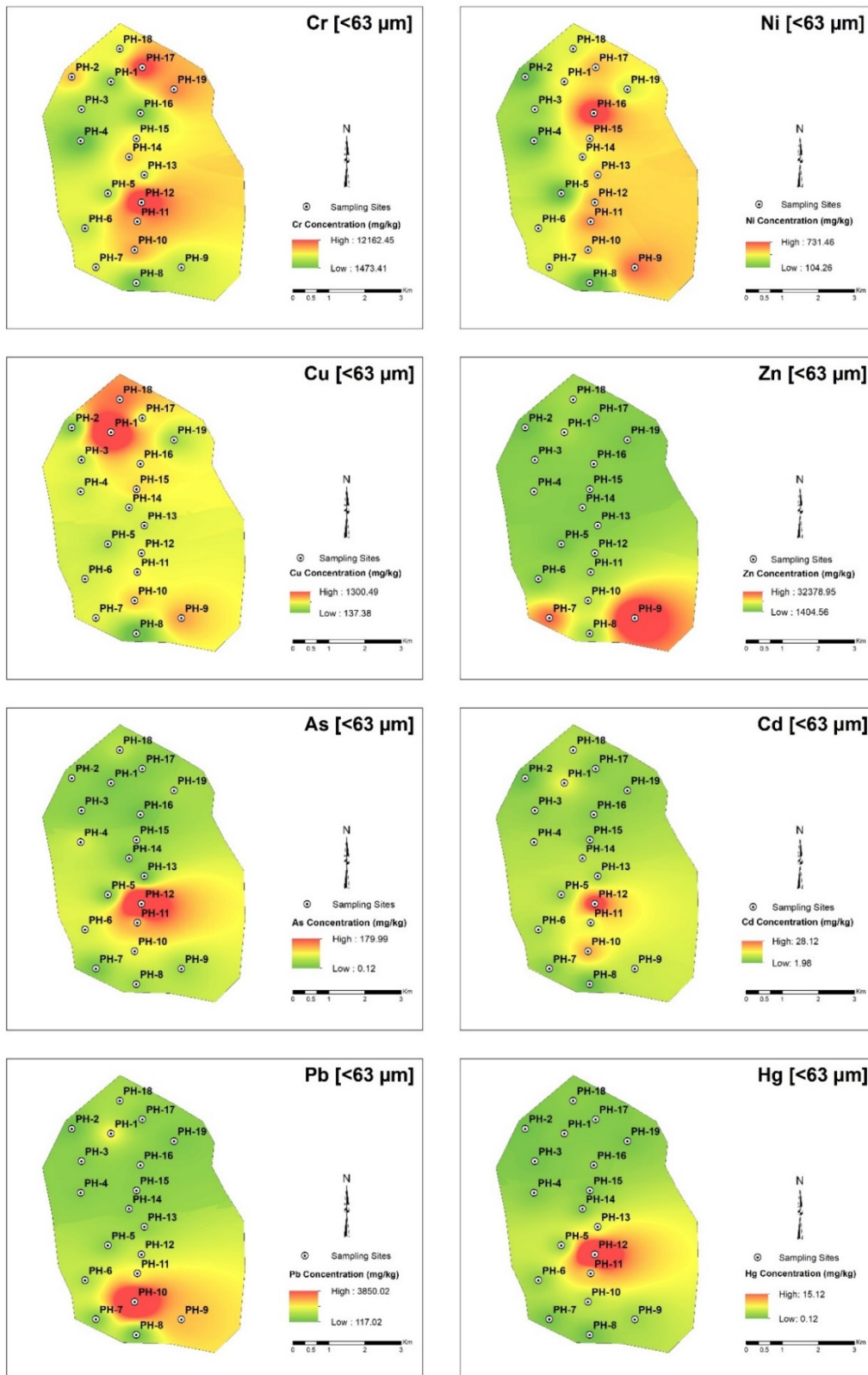


Fig. 2. Spatial distribution of PTEs in road dust ($<63 \mu\text{m}$) from the industrial complex area of Pohang, South Korea.

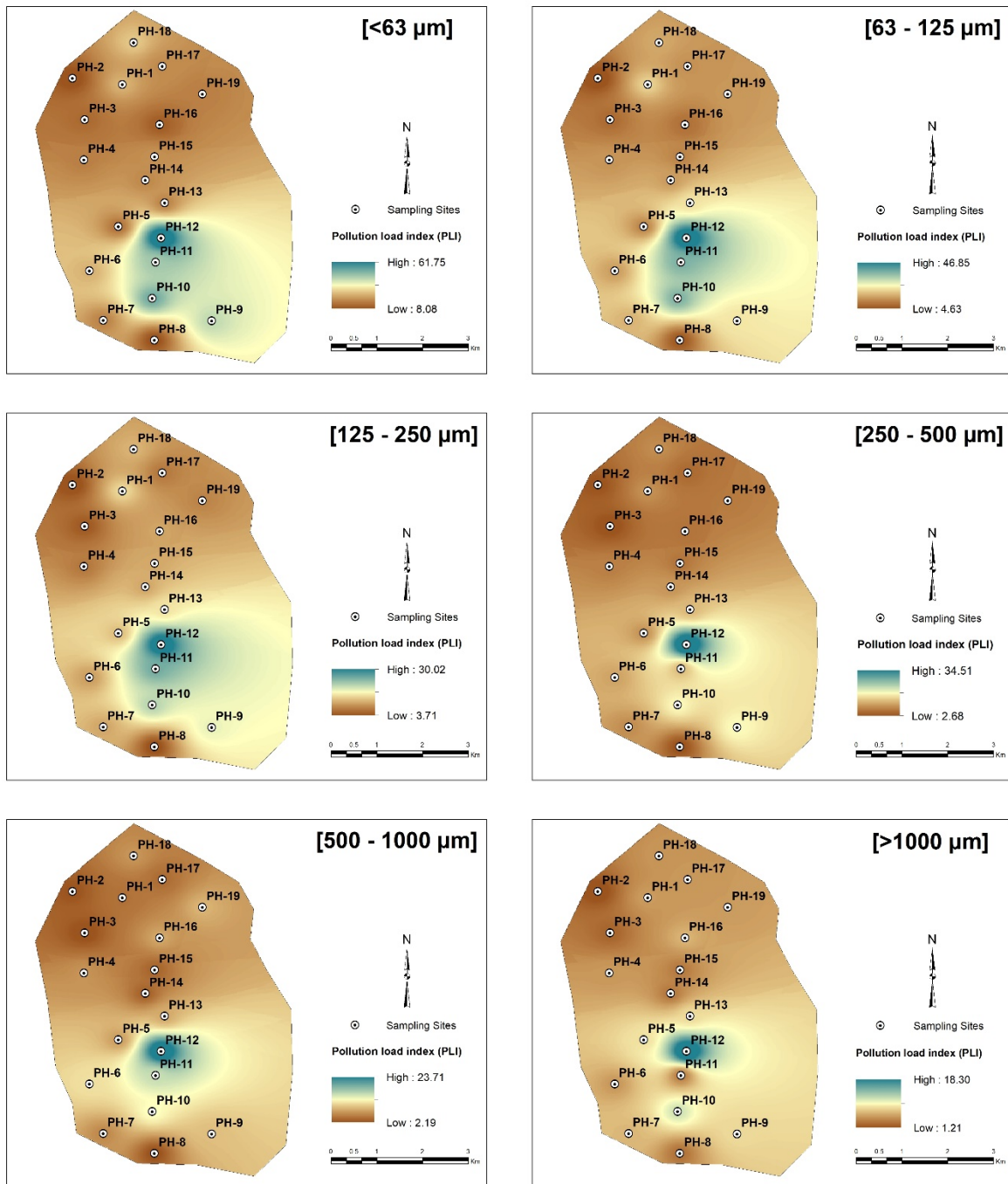


Fig. 3. PLI distribution of each particle size fraction of road dust from the industrial complex area of Pohang, South Korea.

Table 1. Comparison of average PTEs concentrations (mg/kg) (minimum and maximum concentrations in parentheses) in different particle sizes of road dust in this study and those in other published data.

Region	Land use	Size (um)	Cr	Ni	Cu	Zn	As	Cd	Pb	Hg	References
Pohang, South Korea	Industrial	>1000	3474 (955-8851)	131.3 (14.4-921.3)	232.8 (61.7-918.4)	733.4 (153.6-2536.0)	14.3 (0.7-76.9)	1.24 (0.25-5.26)	142.7 (11.2-521.3)	0.22 (0.01-2.27)	This study
		500-1000	2731 (551-7212)	180.1 (15.0-1066.0)	297.9 (73.7-1568.7)	949.2 (242.0-2945.9)	18.6 (0.2-59.1)	1.74 (0.32-11.90)	180.0 (50.5-485.5)	0.42 (0.01-5.54)	This study
		250-500	2917 (590-6939)	149.3 (23.1-350.8)	326.2 (55.1-1077.3)	1302.0 (334.3-3543.7)	16.2 (0.1-77.6)	2.65 (0.40-15.44)	234.3 (47.8-708.1)	0.56 (0.01-6.87)	This study
		125-250	3420 (750-8702)	213.1 (38.5-545.6)	287.7 (74.4-486.7)	1897.1 (464.1-4425.1)	13.7 (3.2-24.2)	3.43 (0.53-20.65)	250.8 (84.0-723.6)	0.81 (0.03-9.04)	This study
		63-125	4664 (1478-9690)	343.0 (70.1-949.0)	414.1 (168.6-920.5)	3145.4 (1023.0-8938.4)	17.3 (0.4-78.9)	5.23 (0.80-19.71)	395.5 (76.5-1534.1)	1.10 (0.06-10.72)	This study
		<63	5225 (1473-12162)	352.6 (104.3-731.5)	460.9 (137.4-731.5)	6161.4 (1404.6-32379.0)	23.2 (0.1-180.0)	7.43 (1.35-28.13)	644.5 (117.0-3850.0)	1.69 (0.12-15.12)	This study
Onsan, South Korea	Industrial	<63	596 (200-1416)	364 (106-1081)	7071 (975-181879)	34592 (4400-166457)	961 (110-2721)	225.1 (1706-975.6)	13561 (1253-44667)	17.0 (1.2-45.1)	Jeong et al. 2021
Viana do Castelo, Portugal	Industrial	<10	296 (BDL-762)	110 (BDL-318)	1816 (617-4669)	2162 (BDL-3819)	100 (41.0-165)	-	276 (109-545)	-	Alves et al. 2020
Huainan, China	Industrial	<75	83 (26-1300)	-	57 (9.8-490)	830 (72-8700)	-	0.64 (0.13-1.8)	71 (16-1000)	0.26 (0.027-2.3)	Liu et al. 2021
Tongchuan, China	Industrial	<75	106.4	25.3	32.6	141.8	6.7	-	74.9	-	Lu et al. 2017
Busan, South Korea	Urban	<63	92.2 (11.4-698)	15.6 (5.5-46.0)	80.7 (14.4-636)	430 (127-948)	13.3 (5.8-88.4)	1.1 (0.3-6.8)	85.3 (19.7-500)	0.01 (0.01-0.02)	Jeong and Ra 2022b
Dhaka, Bangladesh	Urban	<74	144.34 (108.9-199.42)	37.01 (25.44-56.58)	49.68 (30.23-74.44)	239.16 (107.56-683.23)	8.09 (5.16-11.74)	11.64 (6.08-21.52)	18.99 (9.07-43.19)	-	Safiur Rahman et al. 2019
Delhi, India	Urban	<75	148.8	36.4	191.7	284.5	-	2.65	120.7	-	Suryawanshi 2016
Jeddah, Saudi Arabia	Urban	<63	65.43 (42.44-101.00)	11.66 (32.00-77.00)	139.11 (86.00-211.00)	487.52 (304.72-736.00)	21.55 (13.30-31.03)	7.46 (4.67-11.10)	140.73 (85.00-213.00)	-	Shabbaj et al. 2018
Soil pollution concern standards for road and factory sites of South Korea			40 (Cr ⁶⁺)	500	2000	2000	200	60	700	20	MGL 2019
Soil pollution countermeasure standards for road and factory sites of South Korea			120 (Cr ⁶⁺)	1500	6000	5000	600	180	2100	60	MGL 2019

Table 2. Classification of the pollution levels using mean I_{geo} values for PTEs in six particle size fractions of road dust in this study.

	Cr	Ni	Cu	Zn	As	Cd	Pb	Hg
>1000 μm	4.3	0.3	2.1	2.5	0.1	2.6	1.6	-0.5
500-1000 μm	4.0	0.6	2.4	2.9	0.5	2.9	2.4	0.2
250-500 μm	4.1	0.9	2.7	3.5	0.2	3.6	2.8	1.0
125-250 μm	4.4	1.4	2.6	4.1	0.7	4.1	3.0	1.8
63-125 μm	4.9	2.1	3.2	4.8	0.4	4.9	3.6	2.5
<63 μm	5.1	2.3	3.3	5.4	0.3	5.4	4.1	3.3

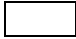






 $I_{geo}<0$; no pollution	 $0<I_{geo}<1$; no pollution to moderate pollution
 $1<I_{geo}<2$; moderate pollution	 $2<I_{geo}<3$; moderate to high pollution
 $3<I_{geo}<4$; high pollution	 $4<I_{geo}<5$; high to extremely high pollution
 $I_{geo}>5$; extremely high pollution	

Table 3. Non-carcinogenic health risk assessment in the [$<63 \mu\text{m}$] size fraction of road dust in this study.

	Adult				Children			
	HQ _{ing}	HQ _{inh}	HQ _{derm}	HI	HQ _{ing}	HQ _{inh}	HQ _{derm}	HI
Cr	6.1×10^{-1}	4.9×10^{-2}	7.0×10^{-1}	1.4	5.7	4.6×10^{-1}	1.6	7.8
Ni	6.2×10^{-3}	4.7×10^{-6}	5.2×10^{-4}	6.7×10^{-3}	5.8×10^{-2}	4.4×10^{-5}	1.2×10^{-3}	5.9×10^{-2}
Cu	4.1×10^{-3}	3.1×10^{-6}	3.1×10^{-4}	4.4×10^{-3}	3.8×10^{-2}	2.9×10^{-5}	7.1×10^{-4}	3.9×10^{-2}
Zn	7.2×10^{-3}	5.5×10^{-6}	8.2×10^{-4}	8.1×10^{-3}	6.8×10^{-2}	5.1×10^{-5}	1.9×10^{-3}	6.9×10^{-2}
As	2.7×10^{-2}	2.1×10^{-5}	1.5×10^{-3}	2.9×10^{-2}	2.5×10^{-1}	1.9×10^{-4}	3.5×10^{-3}	2.6×10^{-1}
Cd	2.6×10^{-3}	2.0×10^{-6}	6.0×10^{-3}	8.6×10^{-3}	2.4×10^{-2}	1.9×10^{-5}	1.4×10^{-2}	3.8×10^{-2}
Pb	6.5×10^{-2}	4.9×10^{-5}	9.9×10^{-3}	7.5×10^{-2}	6.1×10^{-1}	4.6×10^{-4}	2.3×10^{-2}	6.3×10^{-1}
Hg	2.0×10^{-3}	1.5×10^{-6}	6.5×10^{-4}	2.6×10^{-3}	1.9×10^{-2}	1.4×10^{-5}	1.5×10^{-3}	2.0×10^{-2}

Table 4. Carcinogenic health risk assessment in the [$<63 \mu\text{m}$] size fraction of road dust in this study.

	Adult				Children			
	CR _{ing}	CR _{inh}	CR _{derm}	TCR	CR _{ing}	CR _{inh}	CR _{derm}	TCR
As	9.8×10^{-5}	2.7×10^{-11}	2.2×10^{-5}	1.2×10^{-4}	9.2×10^{-4}	2.5×10^{-10}	5.1×10^{-5}	9.7×10^{-4}
Cd	3.9×10^{-5}	3.6×10^{-12}		3.9×10^{-5}	3.7×10^{-4}	3.3×10^{-11}		3.7×10^{-4}
Ni	1.1×10^{-4}	2.3×10^{-11}		1.1×10^{-4}	1.0×10^{-3}	2.1×10^{-10}		1.0×10^{-3}
Pb	9.5×10^{-6}	2.1×10^{-12}	2.2×10^{-6}	1.2×10^{-5}	8.9×10^{-5}	1.9×10^{-11}	5.0×10^{-6}	9.4×10^{-5}